

## Effect of attachment site on stability of cleavable antibody drug conjugates

Magdalena Dorywalska<sup>1,3</sup>, Pavel Strop<sup>1,3</sup>, Jody A. Melton-Witt<sup>1</sup>, Adela Hasa-Moreno<sup>1</sup>, Santiago E. Farias<sup>1</sup>, Meritxell Galindo Casas<sup>1</sup>, Kathy Delaria<sup>1</sup>, Victor Lui<sup>1</sup>, Kris Poulsen<sup>1</sup>, Carole Loo<sup>1</sup>, Stellan Krimm<sup>1</sup>, Gary Bolton<sup>1</sup>, Ludivine Moine<sup>2</sup>, Russell Dushin<sup>2</sup>, Thomas-Toan Tran<sup>1</sup>, Shu-Hui Liu<sup>1</sup>, Mathias Rickert<sup>1</sup>, Davide Foletti<sup>1</sup>, David L. Shelton<sup>1</sup>, Jaume Pons<sup>1</sup>, and Arvind Rajpal<sup>1</sup>

<sup>1</sup>Rinat Laboratories, Pfizer Inc., 230 East Grand Avenue, South San Francisco, CA 94080, USA

<sup>2</sup>Worldwide Medicinal Chemistry, Pfizer Inc., 445 Eastern Point Road, Groton, CT, 06340, USA

<sup>3</sup>These authors contributed equally to the work

## **Supporting Information – Table of Contents**

1. Supplementary Table 1 – Cytotoxicity of untreated and plasma-treated cleavable conjugates against the BxPC3 cell line (M1S1+++).
2. Supplementary Table 2 – Inhibition of Cathepsin B-catalyzed cleavage of the C16 Site A-C6-VC-PABC-Aur0101 substrate upon addition of mouse or human plasma.
3. Supplementary Figure 1 – Stability analysis of the cleavable C16 Site A-C6-VC-PABC-Aur0101 conjugate using hydrophobic interaction chromatography.
4. Supplementary Figure 2 – Mass spectrometric analysis of the cleavage product of C16 Site A-C6-VC-PABC-Aur0101 conjugate isolated from mouse plasma.
5. Supplementary Figure 3 – Cytotoxicity assays of cleavable C6-VC-PABC-Aur0101 conjugates across various sites.
6. Supplementary Figure 4 – Correlation between changes in IC<sub>50</sub> values (efficacy) and changes in DAR (stability) for cleavable conjugates incubated in mouse plasma.
7. Supplementary Figure 5 – Pharmacokinetic profiles of the humanized C16 Site D-C6-VC-PABC-MMAD conjugate in rat, and the chimeric C16 Site D-C6-VC-PABC-MMAD conjugate in cynomolgus monkey.

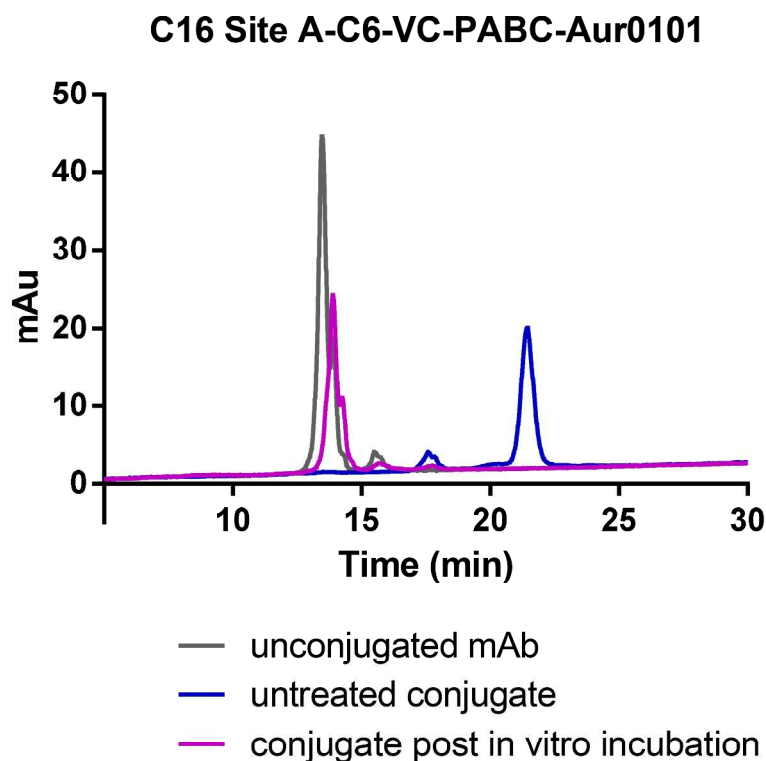
**Supplementary Table 1.** Cytotoxicity of untreated and plasma-treated cleavable conjugates against the BxPC3 cell line (M1S1+++).

Conjugate	Max DAR	Actual DAR	IC50 [nM] untreated conjugate	IC50 [nM] plasma treated conjugate
C16 Site A-C6-VC-PABC-Aur0101	2.0	1.9	1.2	≥ 266
C16 Site B-C6-VC-PABC-Aur0101	2.0	1.8	1.0	12.0
C16 Site C-C6-VC-PABC-Aur0101	2.0	1.5	0.8	3.8
C16 Site D-C6-VC-PABC-Aur0101	2.0	2.0	1.1	6.1
C16 Site E-C6-VC-PABC-Aur0101	2.0	1.7	0.9	3.0
C16 Site F-C6-VC-PABC-Aur0101	2.0	1.9	1.0	1.4
C16 Site G-C6-VC-PABC-Aur0101	2.0	1.9	0.9	0.9
C16 Site H-C6-VC-PABC-Aur0101	4.0	3.9	0.6	0.8
C16 Site I-C6-VC-PABC-Aur0101	2.0	2.0	1.0	0.9
NCC Site F-C6-VC-PABC-Aur0101	2.0	2.0	N/A	-

**Supplementary Table 2.** Inhibition of Cathepsin B-catalyzed cleavage of the C16 Site A-C6-VC-PABC-Aur0101 substrate upon addition of mouse or human plasma. The VC-PABC cleavage activity is expressed in terms of ADC stability values which are shown as percentage. Pefabloc was added to mouse plasma to inhibit the activity of endogenous plasma enzyme. Please refer to Table 2 for demonstration that Pefabloc alone does not affect Cathepsin B activity.

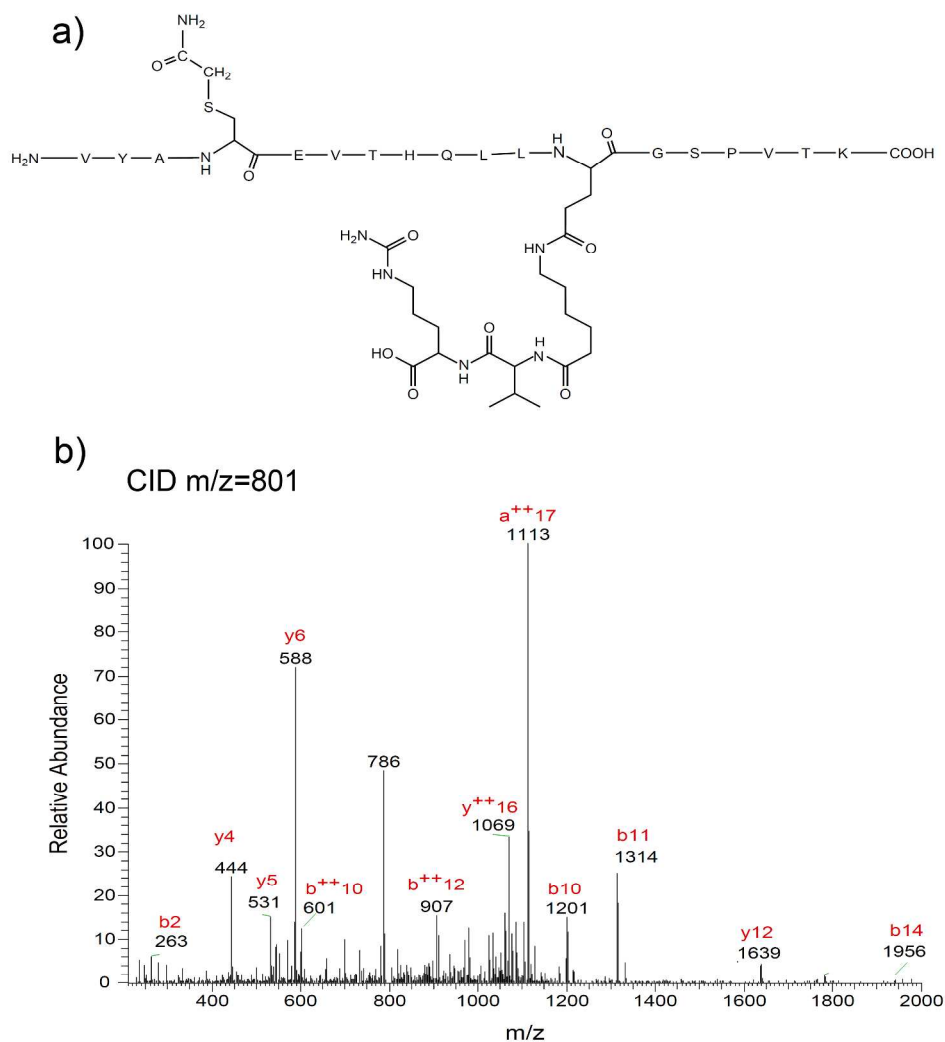
pH	Additive	Mouse Cathepsin B stability (%)	Human Cathepsin B stability (%)
6.0	-	0	0
6.0	Human plasma	100	100
6.0	Mouse plasma & Pefabloc, 1 mM	99	99

Supplementary Figure 1



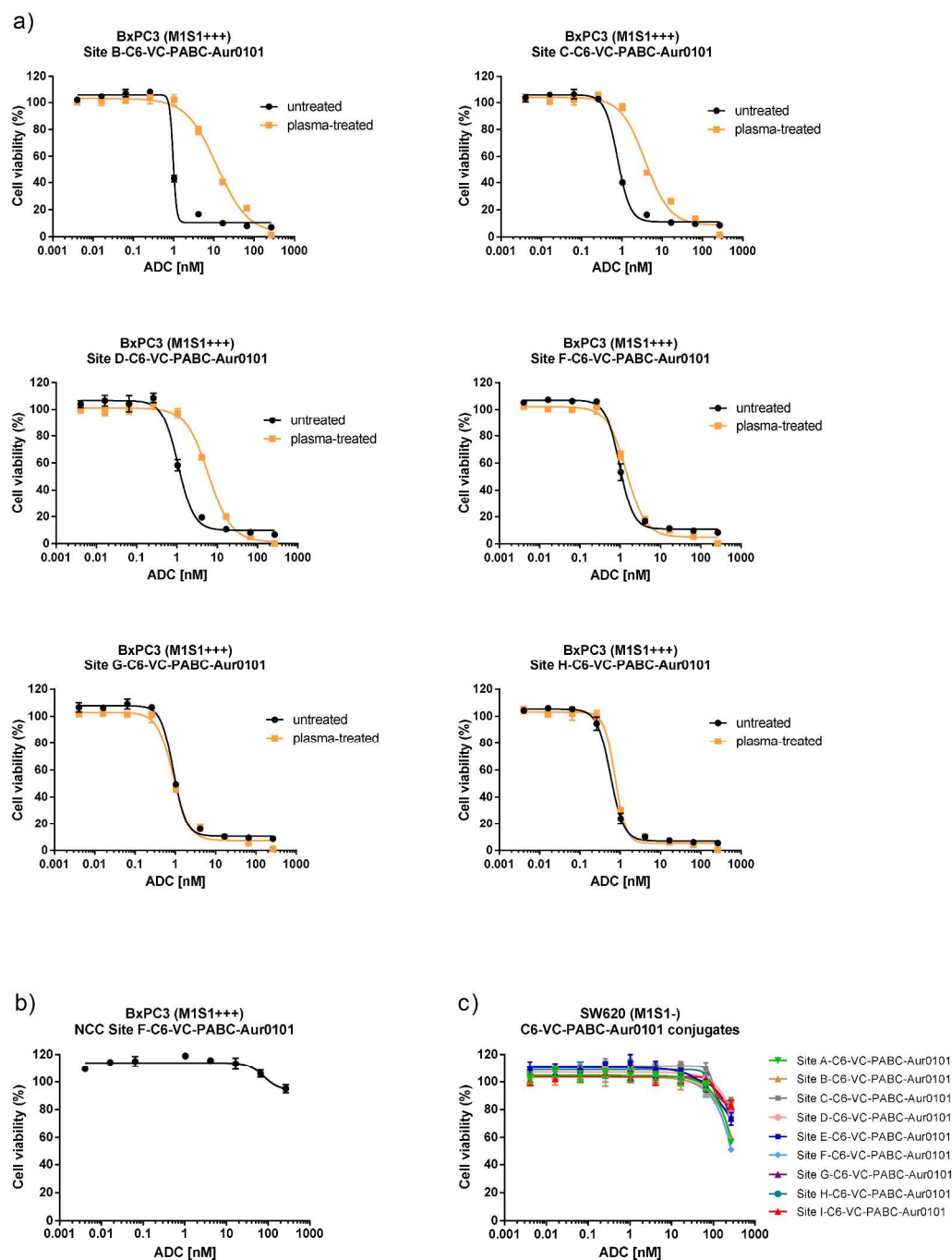
**Supplementary Figure 1.** Stability analysis of the cleavable C16 Site A-C6-VC-PABC-Aur0101 conjugate using hydrophobic interaction chromatography (HIC). Chromatograms show the tagged C16 antibody prior to conjugation (gray line), the C16 Site A-C6-VC-PABC-Aur0101 conjugate before *in vitro* plasma treatment (blue line), and the conjugate purified following plasma incubation (purple line) as described. Changes in the conjugate retention time correspond to changes in the hydrophobic content of the compounds.

## Supplementary Figure 2



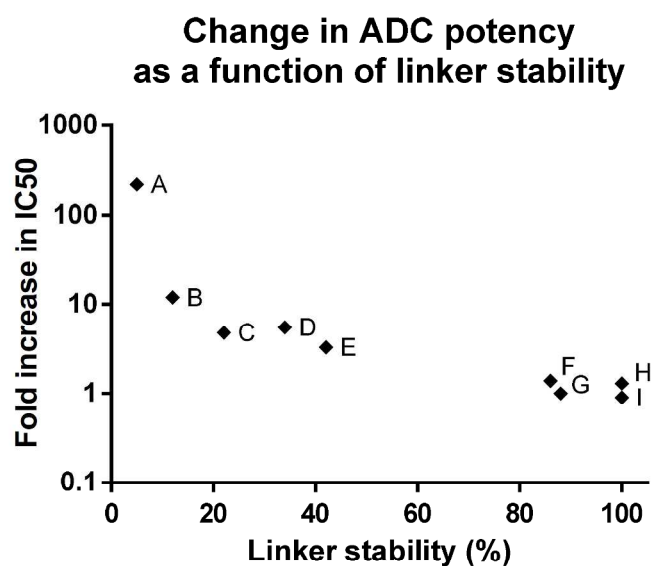
**Supplementary Figure 2.** Mass spectrometric analysis of the cleavage product of C16 Site A-C6-VC-PABC-Aur0101 conjugate isolated from mouse plasma. After plasma incubation, the ADC was purified and subjected to tryptic digestion. a) Predicted molecular structure of tryptic peptide containing glutamine tag on Site A linked to C6-VC. b) The CID spectrum of the precursor ion (+4 charge state,  $m/z=801$ ) shows the y, b and a fragment ions series that matches the amino acid sequence of the predicted structure.

Supplementary Figure 3



**Supplementary Figure 3.** Cytotoxicity assays of cleavable C6-VC-PABC-Aur0101 conjugates across various sites. a) Comparison of *in vitro* cytotoxicity of a series of untreated and plasma-treated C16 C6-VC-PABC-Aur0101 conjugates against high target-expressing BxPC3 cell line (M1S1+++). b) Negative control conjugate NCC Site F-C6-VC-PABC-Aur0101 tested against BxPC3 cells. c) Untreated C16 C6-VC-PABC-Aur0101 conjugate series tested against target-negative SW620 cell line to evaluate their target specificity.

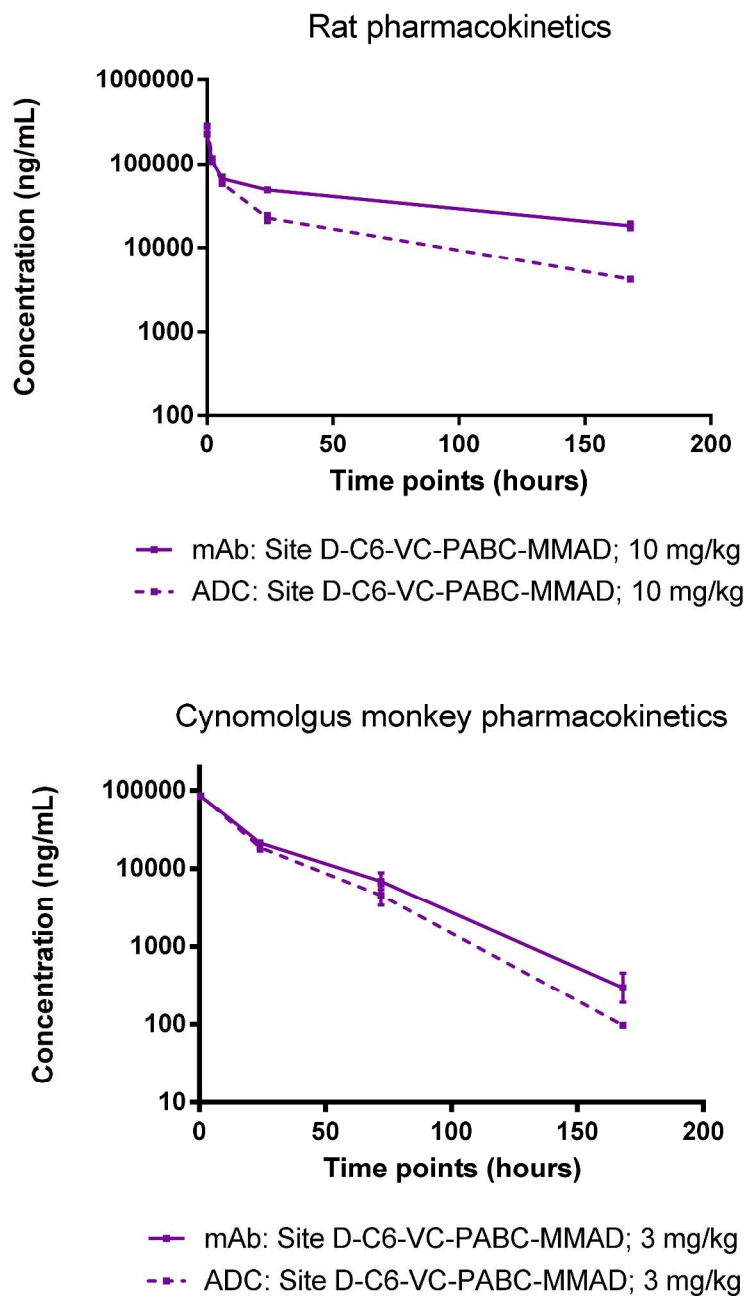
Supplementary Figure 4



**Supplementary Figure 4.** Correlation between changes in IC<sub>50</sub> values (efficacy) and changes in DAR (stability) for cleavable conjugates incubated in mouse plasma. Stability values are calculated as the ratio of drug loading after treatment and before treatment, and expressed as a percentage. Individual data points represent the conjugation sites harboring the C6-VC-PABC-Aur0101 linker-payload.



Supplementary Figure 5



**Supplementary Figure 5.** Pharmacokinetic profiles of a) the humanized C16 Site D-C6-VC-PABC-MMAD conjugate in rat, and b) the chimeric C16 Site D-C6-VC-PABC-MMAD conjugate in cynomolgus monkey. Solid lines represent total antibody ELISA, while dashed lines show anti-drug ELISA. Compounds were dosed at 10 mg/kg or 3 mg/kg, as indicated. The limit of quantitation was 150 ng/mL.